The finite-element method for energy eigenvalues of quantum mechanical systems

L. R. Ram-Mohan, Sunil Saigal, Don Dossa, and J. Shertzer

Citation: Computers in Physics **4**, 50 (1990); doi: 10.1063/1.168374
View online: https://doi.org/10.1063/1.168374
View Table of Contents: https://aip.scitation.org/toc/cip/4/1
Published by the American Institute of Physics

The finite-element method for energy eigenvalues of quantum mechanical systems

L. R. Ram-Mohan
Department of Physics, Worcester Polytechnic Institute, Worcester, Massachusetts 01609

Sunil Saigal
Department of Mechanical Engineering, Worcester Polytechnic Institute, Worcester, Massachusetts 01609

Don Dossa
Department of Physics, Worcester Polytechnic Institute, Worcester, Massachusetts 01609

J. Shertzer
College of the Holy Cross, Worcester, Massachusetts 01610

(Received 26 September 1988; accepted 18 September 1989)

The finite-element method provides a convenient and flexible procedure for the calculation of energy eigenvalues of quantum mechanical systems. The levels of accuracy that can be attained in the method of finite elements are investigated using various approximations. This is illustrated by first considering two classic examples that form a convenient basis for describing the calculational technique: the radial equation for the hydrogen atom for spherically symmetric states and the simple harmonic oscillator problem in one dimension. These two illustrative examples provide guidelines in the calculation of the energy levels of the hydrogen atom in an arbitrary spatially uniform magnetic field, a problem not solvable by analytical means. The results obtained for the $1s_0$ and $2s_0$ levels are the most accurate reported so far. This application shows that finite-element analysis can be employed with advantage for obtaining very accurate results for the energy levels and wavefunctions for quantum mechanical systems.

INTRODUCTION

Over the past three decades, the availability of high-speed computers has facilitated the evolution of the finite-element method (FEM) for the analysis of complex systems in structural mechanics.[1] The general technique of FEM has permeated to other branches of engineering and science as a method for the solution of partial and nonlinear differential equations; for example, the areas of fluid mechanics and atmospheric modeling today rely heavily on FEM. The basic idea of the FEM is to break up the region of interest in the problem into small elements, in each of which the dynamical considerations of the original region are applicable. By decreasing the element size, or by increasing the degree of the interpolation functions, it is possible to improve systematically the accuracy of the analysis; at the same time, it is also possible to accommodate effectively the presence of complicated boundary conditions. A number of refinements to this simple procedure result in numerical calculations that have a high degree of accuracy.

We illustrate the FEM by first considering two simple examples in quantum mechanics. In Sec. I, we solve the radial Schrödinger's equation for s states of the hydrogen atom.[2] We then show how to improve systematically the accuracy of the results for the eigenvalues and the eigenfunctions by refining the grid and increasing the degree of the interpolation functions. In Sec. II, we apply the same technique to the problem of the quantum mechanical one-dimensional simple harmonic oscillator[2] which has Gaussian wavefunctions and again show that a high degree of accuracy is attainable using this method.

In addition to illustrating the FEM, these two examples are relevant to the problem we address in Sec. III: the solution of Schrödinger's equation for hydrogen in an external magnetic field. For weak fields, the wavefunction is similar to that for hydrogen in the absence of a field. In the strong field limit, the wavefunction behaves like a Gaussian in the plane perpendicular to the magnetic field; parallel to the field the wavefunction is still basically "hydrogenlike." Hence this problem displays features of both the simple harmonic oscillator and the hydrogen atom with no external field.

The problem of the hydrogen atom in a magnetic field is an old one. It cannot be solved analytically, essentially because the spherical symmetry of the Coulomb potential is broken by the presence of the external magnetic field. The Hamiltonian is not separable in spherical or cylindrical coordinates, although the latter are more convenient for numerical calculations in the high field regime. The problem of hydrogenlike systems in a magnetic field has arisen in atomic, astrophysical, and solid-state contexts, and there is a long history in the literature of attempts at solving this problem by perturbative and variational methods.[3–10] Using these methods, numerically accurate solutions have

been obtained in the two domains corresponding to very low or very high magnetic fields. In the former, the magnetic field, being small, can be treated as a perturbation, while for high magnetic fields the Coulomb potential can be treated as a perturbation on the energy levels of the electron moving in a magnetic field. Unfortunately, most of these methods fail when the Coulomb energy and magnetic energy are comparable, i.e., in the transition from a hydrogenlike wavefunction to a Gaussian type wavefunction (in the plane perpendicular to the field).[7,9]

In Sec. III we show that the results given by the FEM in the intermediate region, where the Coulomb energy is comparable with the cyclotron energy of the electron in the magnetic field, are extremely accurate. In fact, we can obtain the energies and wavefunctions for the $1s_0$ and $2s_0$ states in fields from 10^5–10^{12} G with an accuracy of better than 1 part in 10^5. This is a direct consequence of using local interpolation functions rather than a global basis set (hydrogenic states or Gaussian states). The results obtained using FEM for the ground state alone were presented by one of us earlier.[11] We conclude with further comments about the advantages of the FEM over conventional variational approaches.

I. THE ENERGY LEVELS OF THE HYDROGEN ATOM

A. A linear interpolation approach

We begin with the time-independent Schrödinger equation[2] for the electron in the hydrogen atom moving in the Coulomb potential of the proton,

$$-(\hbar^2/2m)\nabla^2\Psi_n(\mathbf{r}) - (e^2/r)\Psi_n(\mathbf{r}) = E_n\Psi_n(\mathbf{r}), \tag{1}$$

where the wavefunction of the electron in a stationary state with energy E_n is denoted by $\Psi_n(\mathbf{r})$.

We rescale the radial coordinate r by a_0 (the Bohr radius) and divide Eq. (1) by the energy unit of a Rydberg $R_0(=13.6\text{ eV})$,

$$R_0 = \hbar^2/(2ma_0^2) = e^2/(2a_0), \tag{2}$$

to cast Eq. (1) in dimensionless variables. We retain the same symbol r for the radial coordinate after the rescaling, for convenience, but introduce the symbol ϵ for the reduced energy.

We shall specifically concern ourselves here with spherically symmetric states with zero angular momentum corresponding to the s states with the principal quantum number n. This leads to the equation for the radial wavefunctions $\psi(r)$ given by

$$\left(-\frac{d^2}{dr^2} - \frac{2}{r}\frac{d}{dr} - \frac{2}{r}\right)\psi(r) = \epsilon\psi(r). \tag{3}$$

The physically acceptable solution to the eigenvalue equation must satisfy the boundary condition $\psi(r)\to 0$ as $r\to\infty$.

To implement the FEM, we multiply Eq. (3) by the complex conjugate wavefunction ψ^* and integrate over the radial coordinate r from 0 to ∞. An integration by parts (Green's theorem) of the ψ'' term leads to

$$\int_0^\infty dr\, r^2\left[\psi^{*'}(r)\psi'(r) - \left(\frac{2}{r}\right)\psi^*(r)\psi(r)\right] = \epsilon\int_0^\infty dr\, r^2\psi^*(r)\psi(r). \tag{4}$$

In the present problem, the integration by parts does not provide any "surface" contribution since the boundary is at infinity and the wavefunctions vanish there. However, the FEM being a numerical procedure, the upper limit of the integration has to be set to a finite value, $r = r_c$. This means that we will have a small contribution from the surface term at r_c arising from the integration by parts. The value of r_c is chosen judiciously to reduce this surface term. For example, we could require that the wavefunction be at least six orders of magnitude smaller at r_c than at the origin for the ground state. We return to this issue in Sec. II B below. We now have

$$\int_0^{r_c} dr\, r^2\left[\psi^{*'}(r)\psi'(r) - \left(\frac{2}{r}\right)\psi^*(r)\psi(r)\right] = \epsilon\int_0^{r_c} dr\, r^2\psi^*(r)\psi(r). \tag{5}$$

The integrals in Eq. (5) are discretized into N small one-dimensional elements. In each element n we make the simplest assumption and choose a linear interpolation for the wavefunctions, with the grid points, or nodes, being at the two ends of each element.[1,12] For this linear interpolation we require one input value at the nodal points, which we index by α. For purposes of bookkeeping, we introduce the local coordinate y in any cell. For simplicity we assume that all the elements are of the same size h. The coordinate r in the nth cell is then given by $r = (n-1)\,h + yh$. The unknown wavefunction $\psi(r)$ is assumed to be given at "nodal points" of the nth element where it has the as yet undetermined values $\psi_\alpha^{(n)}$. The wavefunction $\psi(r)$ in the nth element is given by

$$\psi(r) = \sum_{\alpha=1,2}\phi_\alpha\psi_\alpha^{(n)}, \tag{6}$$

where $\phi_1 \equiv (1-y)$ and $\phi_2 \equiv y$ are the linear interpolation functions.

With the assumed linear interpolation for the wavefunction we can directly integrate Eq. (5) in each element and represent the contribution of the nth element to Eq. (5) as a 2×2 local matrix relation:

$$\langle\psi_\alpha^{(n)}|H_{\alpha\beta}^{(n)}|\psi_\beta^{(n)}\rangle = \langle\psi_\alpha^{(n)}|U_{\alpha\beta}^{(n)}|\psi_\beta^{(n)}\rangle, \tag{7}$$

where

$$\begin{aligned} H_{11}^{(n)} &= h(\tfrac{1}{3} - n + n^2) + h^2(\tfrac{1}{2} - \tfrac{2}{3}n), \\ H_{12}^{(n)} &= H_{21}^{(n)} \\ &= h(-\tfrac{1}{3} + n - n^2) + h^2(\tfrac{1}{6} - \tfrac{1}{3}n), \\ H_{22}^{(n)} &= h(\tfrac{1}{3} - n + n^2) + h^2(\tfrac{1}{6} - \tfrac{2}{3}n), \end{aligned} \tag{8}$$

and

$$U_{11}^{(n)} = h^3(\tfrac{1}{5} - \tfrac{1}{2}n + \tfrac{1}{3}n^2),$$

$$U_{12}^{(n)} = U_{21}^{(n)}$$

$$= h^3(\tfrac{1}{20} - \tfrac{1}{6}n + \tfrac{1}{6}n^2),$$

$$U_{22}^{(n)} = h^3(\tfrac{1}{30} - \tfrac{1}{6}n + \tfrac{1}{3}n^2). \quad (9)$$

In deriving Eqs. (8) and (9) use is made of the fact that the derivative $d/dr = (1/h)d/dy$ acts on the interpolation functions used in representing the wavefunctions in each element.

The contributions from all the elements are assembled to construct the "global matrices" **H** and **U**. This is done by noting that the diagonal elements of the global matrices (except for the first and the last) are the sum of contributions from adjacent elements. We ensure that the wavefunction is continuous across the element boundaries by requiring that $\psi_{\alpha=2}^{(n)} = \psi_{\alpha=1}^{(n+1)}$. The complete relation Eq. (5) is now obtained as an $(N+1)\times(N+1)$ matrix equation

$$\langle\psi_i|H_{ij}|\psi_j\rangle = \langle\psi_i|U_{ij}|\psi_j\rangle \quad i,j = 1,...,N+1, \quad (10)$$

where the local index $\{(n)\alpha\}$ has been replaced by a global index i.

The quantity $|\psi_i\rangle$ may be called the "nodal representation" of the wavefunction $\psi(r)$.

An eigenvalue equation is derived from Eq. (10) by invoking the variational principle for minimizing the energy and varying the nodal values ψ_i. We then obtain

$$H_{ij}|\psi_j\rangle = \epsilon U_{ij}|\psi_j\rangle. \quad (11)$$

This generalized eigenvalue problem, Eq. (11), is solved using standard numerical procedures available in numerical anlaysis packages, for the eigenvalues and the corresponding eigenfunctions. The lowest four eigenvalues are shown in Table I, and the wavefunctions for the lowest three energy levels are shown in Fig. 1, corresponding to the ground state of the hydrogen atom and the first two excited states (evaluated with 200 finite elements for a range of $100a_0$ using linear interpolation functions in each element). The analytical result is represented by the continuous curves, and the FEM results are the data points in Fig. 1. The eigenfunctions are not normalized; also, their value at $r = 0$ of unity is merely what is provided by the diagonalization subroutine and is of no special significance.

It is clear from Table I that the linear interpolation functions are not providing a rapid convergence to the analytically known eigenvalues in this problem. We consider below means of improving the accuracy of the procedure.

TABLE I. The energy levels of the hydrogen atom in the FEM with linear interpolation.

Quantum number n	Energy (Rydberg)	Range (a_0)	Number of elements	Exact eigenvalue
1	−0.941 709	20.0	20	−1.000 000
2	−0.238 261			−0.250 000
3	−0.120 321			−0.111 111
4	−0.035 843			−0.062 500
1	−0.997 725	20.0	120	−1.000 000
2	−0.249 607			−0.250 000
3	−0.123 263			−0.111 111
4	−0.044 727			−0.062 500
1	−0.941 709	100.0	100	−1.000 000
2	−0.238 203			−0.250 000
3	−0.106 764			−0.111 111
4	−0.060 446			−0.062 500
1	−0.997 725	100.0	600	−1.000 000
2	−0.249 571			−0.250 000
3	−0.110 957			−0.111 111
4	−0.062 428			−0.062 500

B. Improving accuracy in the FEM

There are two basic schemes for improving the accuracy in the FEM: increasing the degree of the interpolation functions, and refining the grid by increasing the cutoff or the number of elements.

To go beyond the approximation of linear interpolation, we can employ higher-order Lagrange polynomials in each element by providing a larger number of nodes in each element. Given the general exponential decay form of the solutions for the present problem we should expect that increasing the number of elements or the degree of the polynomial will improve matters steadily. For faster convergence, we could attempt to ensure that the continuity of the function ψ *as well as* its derivatives be maintained across the element boundaries. For a system with propagating states the continuity of the first derivative of ψ has physical meaning in quantum mechanics through the fact that the "probability current" is conserved across inter-

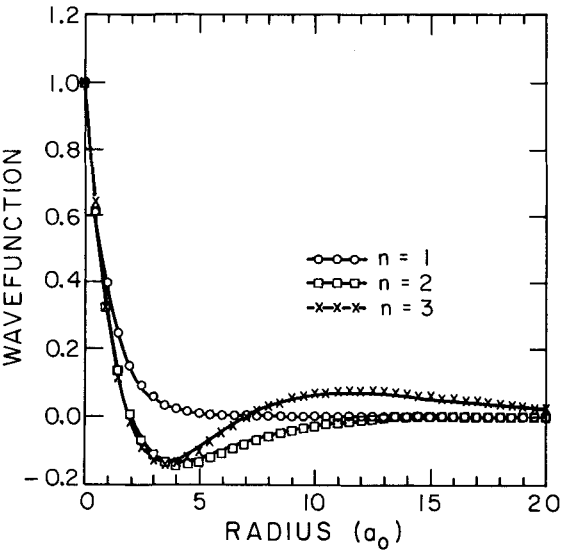

FIG. 1. The radial wavefunctions for the lowest three spherically symmetric states of the hydrogen atom. The data points are those obtained by the FEM using linear interpolation in 200 elements, while the continuous curves are the analytical, exact solutions. The wavefunctions have not been normalized to unity.

faces. For bound-state problems with states stationary in time the continuity of the first derivative of the wavefunction across the element boundaries is required by the fact that Schrödinger's equation is of second order. In fact, we can require that the first *and* the second derivative of the wavefunction be continuous across the element boundaries. We can therefore use the fact that the wavefunctions have continuous first and second derivatives, and represent ψ with Hermite interpolation polynomials that are the appropriate polynomials for ensuring that ψ and its derivatives are continuous at the element boundaries. (These Hermite interpolation polynomials should not be confused with the Hermite polynomial functions that occur in the quantum mechanical simple harmonic oscillator problem. The usual definition of Hermite interpolation polynomials is being extended here to include those with continuity in the second derivative as well.) We show in the Appendix how these interpolation functions can be derived.

For example, consider the case where continuity of the wavefunction and its first two derivatives across element boundaries is imposed. In the nth element the wavefunction can be expressed as

$$\psi(r) = \sum_{\alpha} [\phi_{\alpha}(r)\psi_{\alpha}^{(n)} + \bar{\phi}_{\alpha}(r)\psi_{\alpha}'^{(n)} + \bar{\bar{\phi}}_{\alpha}(r)\psi_{\alpha}''^{(n)}], \quad (12)$$

where α is the node index within the nth element, $\phi_{\alpha}(r)$, $\bar{\phi}_{\alpha}(r)$, $\bar{\bar{\phi}}_{\alpha}(r)$ are Hermite interpolation functions, and $\psi_{\alpha}'^{(n)}$, $\psi_{\alpha}''^{(n)}$ are the as yet undetermined derivatives of ψ defined at the nodal points α in element n. The contributions of the individual finite elements to the total integral relation of Eq. (5) are obtained by following the procedure outlined above for elements obtained from linear interpolation. Now each node α in element n will have three unknown coefficients $\psi_{\alpha}^{(n)}$, $\psi_{\alpha}'^{(n)}$, and $\psi_{\alpha}''^{(n)}$ associated with it, and the element matrices are now $3\alpha \times 3\alpha$ in dimension. (With linear interpolation the element matrices are 2×2 matrices, since an element n has two nodes, each with just one "degree of freedom" associated with the value of $\psi_{\alpha}^{(n)}$ at the node.) The continuity of the wavefunction and its derivative across the element boundary is ensured by overlaying the element matrices while composing the global matrices of Eq. (10) such that the global matrix elements corresponding to the common nodes at the boundary obtain contributions from the local element matrices on either side of the boundary nodes.

In Table II we present the results for the eigenvalues obtained from the use of Hermite interpolation functions with three degrees of freedom at each node; the degrees of freedom here refer to the values of $\psi_{\alpha}^{(n)}$, $\psi_{\alpha}'^{(n)}$, and $\psi_{\alpha}''^{(n)}$ at the node α. The results with three nodes per element with three degrees of freedom at each node are clearly in excellent agreement with the analytical values.

The second issue we address is the effect of varying the cutoff. The range of the integration in the problem is from zero to infinity. This has been approximated by integrating only up to r_c, where r_c has been an adjustable parameter so far. It is found that as the value of r_c is increased, we obtain a larger number of negative eigenvalues corresponding to the bound states in the problem. We can provide a mechanical analogy to the bending of a bar to mimic the behavior of the wavefunction that has $(n-1)$ zeros, where n is the principal quantum number. The kinetic and potential energy terms can be viewed as the "stiffness matrix" of the bar.[1] For a fixed number of elements a shorter bar is more difficult to bend to provide the correct oscillatory shape corresponding to the wavefunction for larger n.

TABLE II. The energy levels of the hydrogen atom using Hermite interpolation in the FEM: range of $100a_0$, number of elements is 50; d.o.f. = degrees of freedom.

Quantum number n	Energy (Rydberg) Two nodes with three d.o.f. per element	Three nodes with three d.o.f. per element	Exact eigenvalue
1	−0.999 999 9	−0.999 999 999 999 9	−1.000 000...
2	−0.249 999 7	−0.250 000 000 000 0	−0.250 000...
3	−0.111 068 8	−0.111 111 111 111 1	−0.111 111...
4	−0.062 483 3	−0.062 500 000 000 9	−0.062 500...
5	−0.039 997 8	−0.040 000 068 132 8	−0.040 000...

The step of integration by parts in Eq. (4) was necessary in the case of linear interpolation functions, as otherwise the second derivative terms would vanish. With the use of polynomials of degree higher than 1 this integration by parts becomes unnecessary, and in this case the approximation of dropping the surface term does not arise. (However, the symmetry of the global matrices may be lost, depending on the nature of the boundary condition at the cutoff.)

Bettess[13] has shown that one can extend the range of the FEM all the way to infinity by attaching an "infinite element" extending from $r = r_c$ to $r = \infty$. The interpolation functions for such an element are taken to be Lagrange interpolation functions multiplied by an appropriate decay factor. In the present application it is natural to choose the functions to be

$$N_{\infty,\alpha} = e^{(r_{\alpha} - r)/L} \prod_{\beta,(\beta \neq \alpha)}^{s} \frac{(r_{\beta} - r)}{(r_{\beta} - r_{\alpha})} . \quad (13)$$

Here, the s points r_{α} extend from r_c to $r = \infty$. The rate of decay of the exponential factor is governed by the scale parameter L, which is chosen to have some reasonable (large) value. We have not included this correction term in our analysis since we have extended the range of integration so as to make the wavefunctions at least 10^{-6} of their value at the origin. The use of the infinite element in quantum mechanical problems with infinite domains is a subject for further exploration in the future.

Before concluding this section on accuracy, a few comments on numerical error from integration and matrix diagonalization are in order. In the two examples addressed in Secs. I and II, all integrations can be performed exactly using four-point Gauss quadrature,[14] since the integrations involve polynomials of degree 7, or less. In the more complicated problem of hydrogen in a magnetic field, the Coulomb potential term cannot be evaluated exactly. Hence the issue of numerical error is an important one. We find that 16-point Gauss quadrature is necessary to guarantee the accuracy of the energy to 1 part in 10^6.

Finally, the matrix diagonalization for the above analysis was done with double precision using the well-tested

and reliable subroutines in the EISPACK subroutine library.[15] For matrices of dimensions larger than, say, 500×500 we resort to a special procedure, the subspace iteration algorithm, which has been developed specifically for finite-element analysis.[1,16] Subspace iteration allows one to calculate the lowest eigenvalues and the corresponding eigenvectors of generalized eigenvalue problems, exploiting the symmetry and bandedness of the matrices. This algorithm was used for the problem of the hydrogen atom in an external magnetic field in Sec. III, which requires two-dimensional FEM techniques and consequently generates large matrices.

II. THE QUANTUM MECHANICAL SIMPLE HARMONIC OSCILLATOR

In this section we present the results of the calculation for the energy eigenvalues for the quantum mechanical simple harmonic oscillator using FEM. The essential computational issues are the same as the ones considered for the hydrogen atom in Secs. I A and I B above. Earlier studies of this problem using FEM did not emphasize the high accuracy obtainable by this method.[17]

We begin with Schrödinger's equation for the oscillator,[2]

$$-\frac{\hbar^2}{2m}\frac{d^2}{dx^2}\psi_n(x)+\frac{1}{2}kx^2\psi_n(x)=E_n\psi_n(x), \quad (14)$$

where k is the spring constant of the oscillator. Let us measure the energy in units of $\lambda=\hbar\omega/2$, where $\omega=\sqrt{k/m}$, so that $E=\epsilon\lambda$. Let us choose the unit of distance to be $\sqrt{\hbar/(m\omega)}$. Schrödinger's equation in dimensionless form is then given by

$$\frac{d^2}{dx^2}\psi(x)+(\epsilon-x^2)\psi(x)=0. \quad (15)$$

We multiply through Eq. (15) by $\psi^*(x)$ and integrate from $-\infty$ to $+\infty$. The integrals are estimated by breaking up the region of integration into finite elements. We find that the range of $[-10,+10]$ provides an adequate representation of the infinite region of interest.

In Tables III and IV we present the results of using various interpolation functions. For linear interpolation (Table III) the eigenvalues do not at all display spectroscopic accuracy; furthermore, the number of eigenvalues that are obtained with errors less than a few percent is rather small. This may be compared with results shown in Table IV obtained using Hermite interpolation functions with two nodes and three degrees of freedom for the same number of elements. The lowest four eigenvalues are accurate to better than six significant figures, and the number of eigenvalues obtained to five significant figures is 36. Finally, with Hermite interpolation with three degrees of freedom and three nodes per element, the first 20 eigenvalues agree with the analytical results to 14 significant figures, and the number of eigenvalues obtained to 5 significant figures or better increases to 40.

We conclude this section by noting that the improvements in the levels of accuracy we have demonstrated by the use of Hermite interpolation have not been reported in the literature for the energy levels of quantum mechanical systems. Our analysis shows that the FEM is a reliable method for the bound-state problems of quantum mechanics.

TABLE III. The energy levels of the one-dimensional simple harmonic oscillator in the FEM with linear interpolation functions. The range used is $-10\leqslant x\leqslant10$, and the number of elements is 60.

Quantum number n	Energy ($\hbar\omega_0/2$)	Exact eigenvalue
0	1.006 93	1.00...
1	3.034 39	3.00...
2	5.088 75	5.00...
3	7.169 42	7.00...

TABLE IV. The energy levels of the one-dimensional simple harmonic oscillator in the FEM using Hermite interpolation with three degrees of freedom (d.o.f.) at each node. Two and three nodes per element have been used. The range used is $-10\leqslant x\leqslant10$, and the number of elements is 60.

Quantum number n	Energy ($\hbar\omega_0/2$)	Exact eigenvalue
	Two nodes with three d.o.f.	
0	1.000 000	1.00...
1	3.000 000	3.00...
2	5.000 000	5.00...
3	7.000 001	7.00...
⋮	⋮	⋮
35	71.000 354	71.00...
36	73.000 391	73.00...
	Three nodes with three d.o.f.	
0	1.000 000 000 000 0	1.00...
1	3.000 000 000 000 0	3.00...
2	5.000 000 000 000 0	5.00...
⋮	⋮	⋮
38	76.999 703	77.00...
39	78.999 173	79.00...

III. THE HYDROGEN ATOM IN AN EXTERNAL MAGNETIC FIELD

Schrödinger's equation for s states of the hydrogen atom in an external magnetic field B along the z direction can be written as

$$\left(\frac{\partial^2}{\partial\rho^2}+\frac{1}{\rho}\frac{\partial}{\partial\rho}+\frac{\partial^2}{\partial z^2}+\frac{2}{\sqrt{\rho^2+z^2}}-\gamma^2\rho^2+2\gamma+\epsilon\right)\times\Psi(\mathbf{r})=0, \quad (16)$$

where $\gamma=1$ corresponds to a magnetic field $B=4.70\times10^9$ G. The term linear in γ arises from the electron's magnetic dipole interacting with the external field with the electron spin oriented downward. The energy is expressed in Rydberg (R_0) units, as before, and we retain the Bohr radius a_0 as the unit of length.

Equation (16) is a nonseparable partial differential equation in the two variables z and ρ. The boundary conditions on the wavefunction are

$$\Psi(\rho\to\infty,z)\to 0,$$
$$\Psi(\rho,z\to\pm\infty)\to 0. \tag{17}$$

We use the FEM to solve Eq. (16) by using a two-dimensional grid, in ρ and z, for the discretization of the problem. Within each two-dimensional element we assign nine nodes: at each of the corners, at midpoints of the sides, and at the center of the element. Hermite interpolation appropriate to nine nodes per element and four degrees of freedom per node is used to represent the wavefunction within each element. The two-dimensional interpolation functions are simply the products of one-dimensional Hermite interpolation polynomials in ρ and in z. We require that Ψ, $\partial\Psi/\partial\rho$, $\partial\Psi/\partial z$, and $\partial^2\Psi/\partial\rho\,\partial z$ be continuous across the boundaries of the elements. A local coordinate system is introduced into each element n which has the range -1 to 1 in both directions. Given that the size of the element is $h_\rho^n \times h_z^n$, it is simple to show that the local coordinates x and y are related to their respective global coordinates ρ and z by

$$\rho=\rho_0^{(n)}+h_\rho^{(n)}(1+x)/2,$$
$$z=z_0^{(n)}+h_z^{(n)}(1+y)/2, \tag{18}$$

where $\rho_0^{(n)}$ and $z_0^{(n)}$ are the global coordinates at the corner $x=-1, y=-1$ of element n. In terms of local coordinates the nodes are located at the points where x and y have the value 0 or ± 1.

The wavefunction in element n is approximated by a sum of products of fifth degree Hermite polynomials in x and y:

$$\Psi^{(n)}(\rho,z)=\sum_{\alpha,\beta=1}^{6}\Psi_\gamma^{(n)}p_\alpha(x)p_\beta(y);\quad \gamma=6(\alpha-1)+\beta. \tag{19}$$

These polynomial interpolates have the special property that the 36 expansion coefficients are the values of Ψ, $\partial\Psi/(\partial\rho)$, $\partial\Psi/(\partial z)$, and $\partial^2\Psi/(\partial\rho\,\partial z)$ at the nine nodes in the element. The Hermite interpolation functions in the nth element are

$$p_1(x)=x^2-1.25x^3-0.5x^4+0.75x^5,$$
$$p_2(x)=h_r^{(n)}(0.25x^2-0.25x^3-0.25x^4+0.25x^5),$$
$$p_3(x)=1-2x^2+x^4,$$
$$p_4(x)=h_r^{(n)}(x-2x^3+x^5),$$
$$p_5(x)=x^2+1.25x^3-0.5x^4-0.75x^5,$$
$$p_6(x)=h_r^{(n)}(-0.5-1.5x+3x^2+5x^3). \tag{20}$$

A procedure for deriving such polynomials is given in the Appendix.

TABLE V. Binding energy of the $1s_0$ state of the hydrogen atom in an external magnetic field. The number of elements is $10\times 10=100$.

B (4.70×10^9 G)	Liu and Starace lower bound upper bound (Rydberg)	Rosner *et al.* lower limit upper limit (Rydberg)	Finite element lower bound (Rydberg)
0.0			0.999 998
5.0×10^{-5}			1.000 098
5.0×10^{-4}		1.000 999	1.000 998
5.0×10^{-3}		1.009 950	1.009 948
0.05	1.094 8	1.095 053	1.095 051
0.5	1.633 4 1.683 6	1.662 338	1.662 336
5.0		3.495 594	3.495 580
50.0	7.472 0 7.605 4	7.578 1 7.580 5	7.579 551
500		15.324 1 15.325 3	15.324 72

The finite-element calculation proceeds along the lines discussed in Secs. I and II. The local elements generate 36×36 matrices whose matrix elements are overlaid to assemble the global matrices. This is done keeping in mind that Ψ and its derivatives have the same values for nodes that are shared by two or four elements.

The cutoff values of the region of interest ρ_c and $\pm z_c$ are determined by requiring that the wavefunctions be at least six orders of magnitude smaller than at the origin. In a magnetic field, Rösner *et al.*[7] have shown that the ground state is compressed in the z direction while the higher excited states are somewhat elongated along the z direction. The asymptotic behavior of the wavefunction in the ρ direction is well represented by the Gaussian form $\exp(-\gamma\rho^2/2)$ in fields $\gamma>1$. Hence the cutoff value ρ_c was adjusted to reflect this behavior with increasing magnetic field. Since the $1s_0$ wavefunction bunches up sharply at the origin with increasing B, we allocated more elements for the region $0<\rho<4a_0$.

Our results for the energies of the $1s_0$ and $2s_0$ states are compared with those of Rösner[7] and of Liu and Starace[9] at various values of the B field in Tables V and VI. Of the

TABLE VI. Binding energy of the $2s_0$ state of the hydrogen atom in an external magnetic field. The number of elements is $10\times 10=100$.

B (4.70×10^9 G)	Liu and Starace lower bound upper bound (Rydberg)	Rosner *et al.* lower limit upper limit (Rydberg)	Finite element lower bound (Rydberg)
0.0			0.249 999
5.0×10^{-5}			0.250 099
5.0×10^{-4}		0.250 993 0	0.250 992
5.0×10^{-3}		0.259 303 1	0.259 302
0.05	0.1746 0.3006	0.296 178 3	0.296 178
0.5	0.2714 0.3188	0.320 937 9	0.320 938
5.0		0.417 77 0.417 98	0.417 902
50.0	0.5110 0.5130	0.512 339 0.512 377	0.512 358
500		0.591 709 9 0.591 718 0	0.591 70

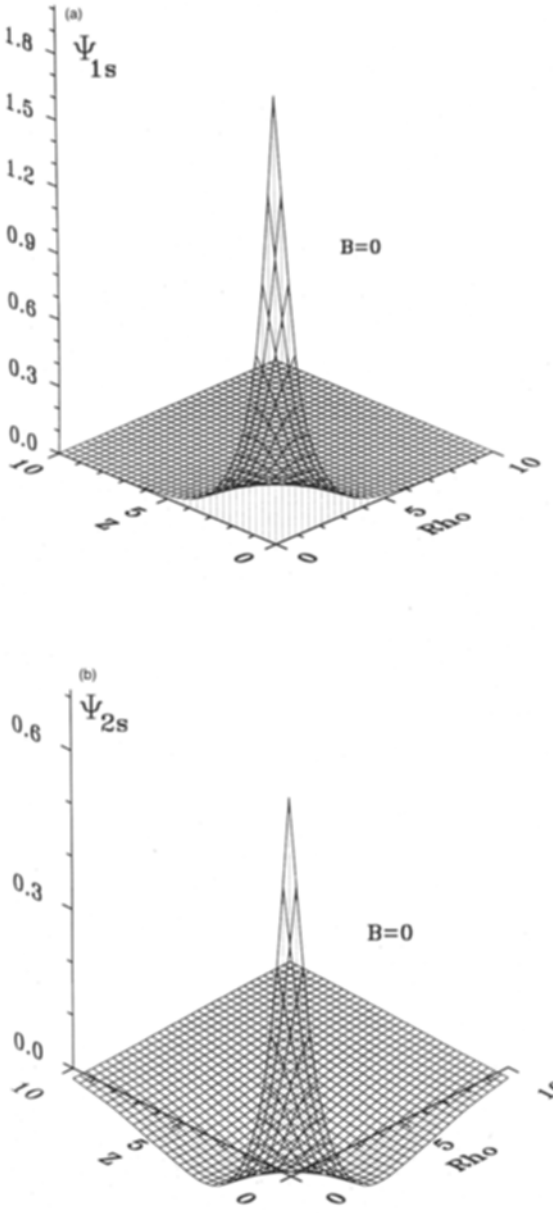

FIG. 2. The normalized s states of the hydrogen atom at zero magnetic field for (a) the $1s_0$ state and (b) the $2s_0$ state.

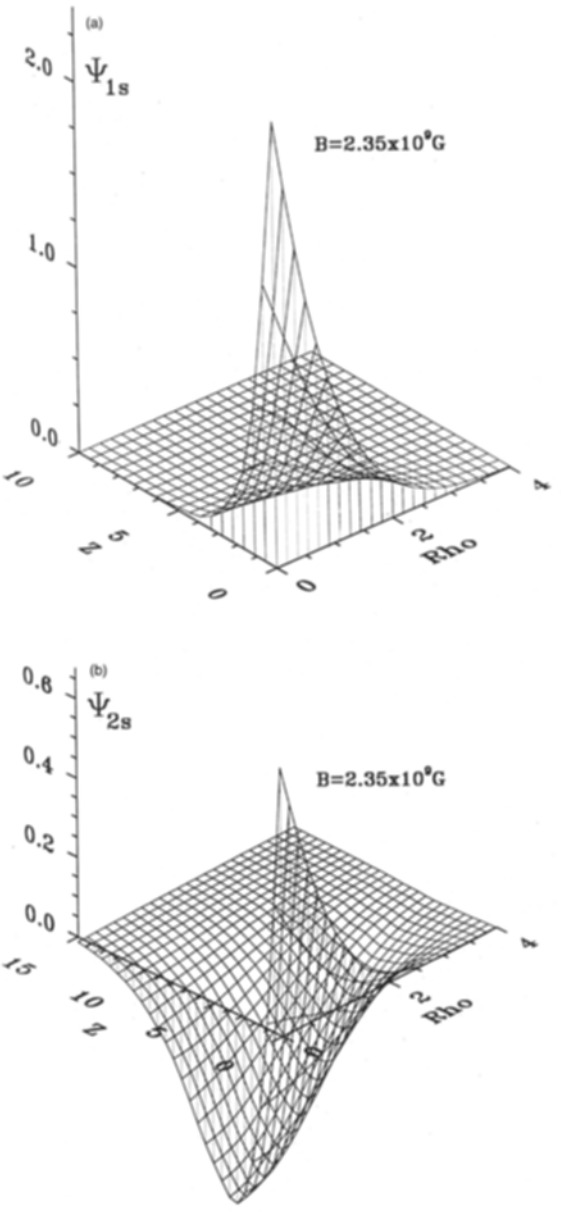

FIG. 3. The normalized s states of the hydrogen atom in a magnetic field of $B = 0.5B_0$ ($B_0 = 4.70\times 10^9$ G) for (a) the $1s_0$ state and (b) the $2s_0$ state.

earlier works only the results of Liu and Starace give a rigorous bound, since they arise from a variational procedure. It is clear that the finite-element results are far superior. The calculation of Rösner *et al.* uses a modified Hartree–Fock approach, which does not guarantee rigorous bounds to the physical energy. Nevertheless, their results agree to six significant digits with the FEM results in fields up to $\gamma = 1$. For higher fields, the finite-element results lie between their upper and lower values. In Figs. 2–4 we provide a two-dimensional display of the wavefunctions at $B = 0$, at $B = 0.5B_0$, and at $B = 50B_0$, where $B_0 = 4.70\times 10^9$ G. The scales along the various axes should be noted in order to appreciate the changes in the wavefunction of the electron produced by the applied magnetic field at these representative values of the B field. It is also interesting to note that the wavefunctions at high fields, shown in Figs. 3 and 4, have nonzero slopes at $\rho = 0$ in the ρ direction. This is due to the fact that the Coulomb potential energy term dominates over the magnetic terms in the Hamiltonian of Eq. (16) very close to the origin even at high magnetic fields. This leads to the deviation from a Gaussian shape for small radial distances.

In conclusion, we note that in this work we have mainly concerned ourselves with (i) the demonstration that the

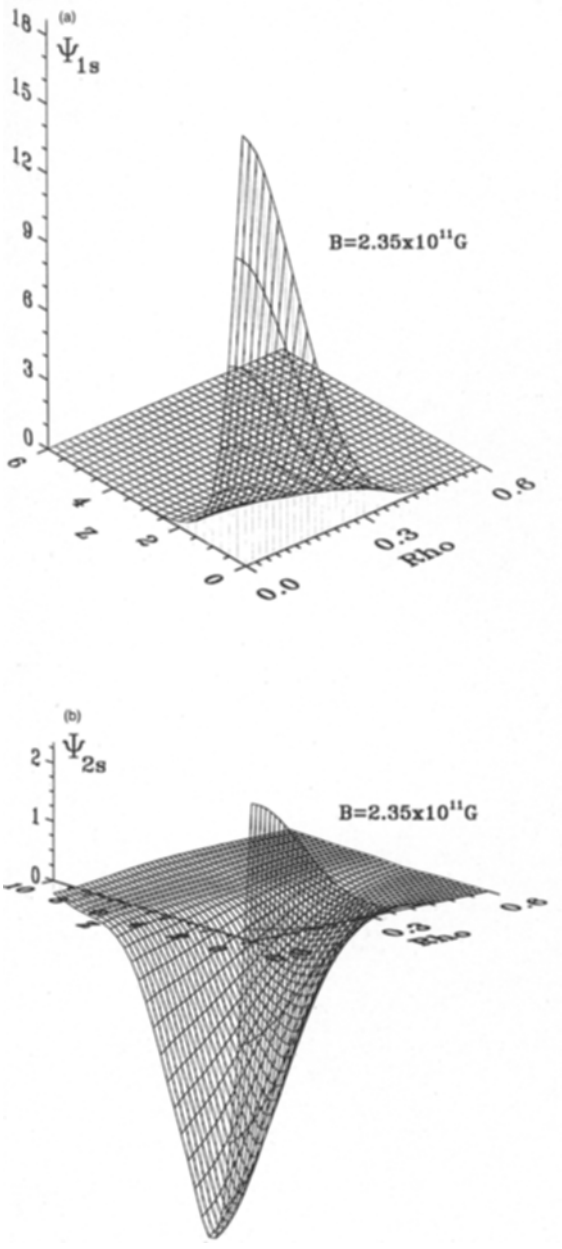

FIG. 4. The normalized s states of the hydrogen atom in a magnetic field of $B = 50B_0$ ($B_0 = 4.70\times 10^9$ G) for (a) the $1s_0$ state and (b) the $2s_0$ state.

FEM is capable of yielding *very accurate* results, by considering two well-known quantum mechanical examples, the radial equation of the hydrogen atom and the one-dimensional simple harmonic oscillator; and (ii) the application of the FEM to a nonseparable partial differential equation, viz., the problem of the hydrogen atom in an external magnetic field. It is of interest to state some of the special features of the FEM. It may be noted that *while the FEM too is a variational method it does not require making accurate guesses at the form of the trial variational solution.* The integration over the finite elements smoothes out the numerical differentiation errors that are expected to occur with the finite-difference method.[12] The singularities in the potential $V(r)\sim 1/r^{\alpha}$, for $0<\alpha\leqslant 2$, do not present any special difficulty for finite elements since $r^2 r^{-\alpha}\,dr$ is bounded, whereas such singularities are problematic within the finite-difference computational schemes for the solution of differential equations. The typical finite elements lead to banded matrices and involve integrations over finite regions, unlike the Rayleigh–Ritz procedures, which involve fully occupied matrices requiring $n(n+1)/2$ integrations for the matrix elements. These banded matrices require less computer memory and also less computational time for obtaining the eigenvalues and eigenfunctions. This also introduces fewer round-off errors in the results since far fewer numerical operations are performed in the algorithm for determining eigenvalues.

The fact that FEM can provide very accurate results for a number of excited states with the use of improved interpolation functions in bound-state problems has not been appreciated earlier, and we expect to see a greater use of the FEM in the solution of physical problems in the future.

ACKNOWLEDGMENTS

One of us (D.D.) has been supported by the Digital Equipment Corporation, Boxboro, Massachusetts 01719. We wish to thank Digital for providing computer resources.

APPENDIX: DERIVATIONS OF THE INTERPOLATION POLYNOMIALS

Here, we display a simple numerical method for generating the Lagrange and the Hermite interpolation polynomials. Let us suppose, without any loss of generality, that the range of interpolation is $[-1,+1]$. This coincides with the range of integration in Gauss–Legendre quadrature. A simple change of variables will allow us to map the region onto any other region [a,b].

1. Lagrange interpolation polynomials

For illustrative purposes, let us evaluate the Lagrange interpolation polynomials for the nodal points $(-1,0,1)$. With three nodal points ($x_\alpha = -1,0,1$) we will have three polynomials, which will be the quadratic functions

$$\phi_\alpha(x) = a_\alpha + b_\alpha x + c_\alpha x^2 \quad (\alpha = 1,2,3), \tag{A1}$$

where $a_\alpha, b_\alpha, c_\alpha$ are coefficients to be determined from the requirement that

$$\phi_\alpha(x_\beta) = \delta_{\alpha,\beta}. \tag{A2}$$

This condition can be written in a matrix form:

$$\begin{bmatrix} 1 & -1 & 1 \\ 1 & 0 & 0 \\ 1 & 1 & 1 \end{bmatrix} \cdot \begin{bmatrix} a_1 & a_2 & a_3 \\ b_1 & b_2 & b_3 \\ c_1 & c_2 & c_3 \end{bmatrix} = \mathbf{I}, \tag{A3}$$

or

$$\mathscr{A}\,\mathscr{B} = \mathrm{I}. \tag{A4}$$

Here, the numerical entries of the matrix $\mathscr{A}$ in the αth row refer to the values of $(1,x,x^2)$ at the nodal points x_α, and $\mathbf{I}$ is the unit matrix. Then the functions ϕ_α are obtained by solving for the coefficients $\mathscr{B} = (a_\alpha,\ldots)$. It is convenient to evaluate numerically the inverse of the matrix $\mathscr{A}$ to identi-

fy the coefficients a_α, b_α, c_α as the *column* entries of the αth column in the inverted matrix. The extension to a larger number of nodes in the range $[-1,1]$ is straightforward.

2. Hermite interpolation polynomials

As an example, let us determine the interpolation functions $\phi_\alpha(x)$, $\overline{\phi_\alpha}(x)$ for the case of two nodes with two degrees of freedom at each node. These functions allow us to write

$$\psi(x) = \sum_\alpha (\phi_\alpha(x)\psi_\alpha + \overline{\phi_\alpha}(x)\psi'_\alpha), \tag{A5}$$

where the Hermite interpolation polynomials $\phi_\alpha(x)$, $\overline{\phi_\alpha}(x)$ must satisfy the conditions

$$\phi_\alpha(x_\beta) = \delta_{\alpha\beta},$$
$$\frac{d}{dx}\,\overline{\phi_\alpha}(x_\beta) = \delta_{\alpha\beta}. \tag{A6}$$

Here, the degrees of freedom refer to the "freedom" in choosing Ψ_α and Ψ'_α.

The general polynomial for the case of two nodes with two degrees of freedom is a cubic that can be written as

$$p_\alpha(x) = a_\alpha + b_\alpha x + c_\alpha x^2 + d_\alpha x^3 \quad (\alpha = 1,...,4). \tag{A7}$$

Here, p_1, p_3 equal ϕ_1, ϕ_3, and p_2, p_4 equal $\overline{\phi_1}$, $\overline{\phi_2}$, respectively. The matrix equation corresponding to Eq. (A3) can be written down with the rows of the matrix on the left being the values of the powers of x at $x = -1, +1$, with the rows arranged alternately for ϕ_α and for $\overline{\phi_\alpha}$. We have

$$\begin{bmatrix} 1 & -1 & 1 & -1 \\ 0 & 1 & -2 & 3 \\ 1 & 1 & 1 & 1 \\ 0 & 1 & 2 & 3 \end{bmatrix} \cdot \begin{bmatrix} a_1 & a_2 & a_3 & a_4 \\ b_1 & b_2 & b_3 & b_4 \\ c_1 & c_2 & c_3 & c_4 \\ d_1 & d_2 & d_3 & d_4 \end{bmatrix} = \mathbf{I}. \tag{A8}$$

Again, an inversion of the matrix allows us to obtain the coefficients a_α, etc., as the numerical entries of the inverted matrix along the αth column.

The numerical method of obtaining the Lagrange and Hermite interpolation polynomials presented here is a convenient and flexible procedure that can be extended in two ways: one is by increasing the number of nodal points in the range $[-1,1]$, and the other is by increasing the number of degrees of freedom.

REFERENCES

1. K.-J. Bathe, *Finite Element Procedures in Engineering Analysis* (Prentice–Hall, Englewood Cliffs, NJ, 1982); T. J. Chung, *Finite Element Analysis in Fluid Dynamics* (McGraw-Hill, New York, 1978); G. Strang and G. Fix, *An Analysis of the Finite Element Method* (Prentice–Hall, Englewood Cliffs, NJ, 1973); O. C. Zienkiewicz and Y. K. Cheung, *Finite Element Methods in Structural and Continuum Mechanics* (McGraw-Hill, New York, 1967); O. C. Zienkiewicz, *The Finite Element Method* (McGraw-Hill, New York, 1977); T. J. R. Hughes, *The Finite Element Method* (Prentice–Hall, Englewood Cliffs, NJ, 1987).
2. L. I. Schiff, *Quantum Mechanics* (McGraw-Hill, New York, 1968), 3rd ed.
3. For a review up to 1977 see R. H. Garstang, Rep. Prog. Phys. **40**, 105 (1977).
4. A. R. P. Rau and L. Spruch, Astrophys. J. **207**, 671 (1976).
5. A. Baldareschi and F. Bassani, in *Proceedings of the 10th International Conference on Physics of Semiconductors*, edited by S. P. Keller, J. C. Hensel, and F. Stern, USAEC Division of Technical Information, Washington, DC (1970), p. 191.
6. C. Aldrich and R. L. Greene, Phys. Status Solidi (B) **93**, 343 (1979).
7. W. Rösner, G. Wunner, H. Herold, and H. Ruder, J. Phys. B **17**, 29 (1984).
8. J. C. Le Guillou and J. Zinn-Justin, Ann. Phys. (NY) **147**, 57 (1983).
9. C. Liu and A. F. Starace, Phys. Rev. A **35**, 647 (1987).
10. C. R. Handy, D. Bessis, G. Sigismondi, and T. D. Morley, Phys. Rev. Lett. **60**, 253 (1988).
11. J. Shertzer, Phys. Rev. A **39**, 3833 (1989).
12. A. Askar, J. Chem. Phys. **62**, 732 (1975); also see M. Friedman, Y. Rosenfeld, A. Rabinovitch, and R. Theiberger, J. Comput. Phys. **26**, 169 (1978).
13. P. Bettes, Int. J. Num. Meth. Eng. **11**, 53 (1977); **15**, 1613 (1980); also see S. Pissanetzky, Int. J. Num. Meth. Eng. **19**, 913 (1983).
14. B. Carnahan, H. A. Luther, and J. O. Wilkes, *Applied Numerical Methods* (Wiley, New York, 1969).
15. B. T. Smith *et al.*, *Matrix Eigensystem Routines—EISPACK Guide*, Lecture Notes in Computer Science, Vol. VI (Springer, New York, 1976), 2nd ed.
16. K.-J. Bathe and E. Wilson, *Numerical Methods in Finite Element Methods* (Prentice–Hall, Englewood Cliffs, NJ, 1976).
17. D. S. Burnett, *Finite Element Analysis* (Addison–Wesley, Reading, MA, 1987), p. 429; also see D. J. Searles and E. I. von Nagy-Felsobuki, Am. J. Phys. **56**, 444 (1988).